Endocytosis of secretory granules in mouse pancreatic β-cells evoked by transient elevation of cytosolic calcium

Lena Eliasson *, Peter Proks †, Carina Ämmälä *, Frances M. Ashcroft †, Krister Bokvist ‡, Erik Renström ‡, Patrik Rorsman ‡§ and Paul A. Smith †

*Department of Physiology and Pharmacology, Division of Medical Biophysics, Medicinaregatan 11, S-413 90 Göteborg, Sweden, † University Laboratory of Physiology, Parks Road, Oxford OX1 3PT, UK and ‡ Department of Islet Cell Physiology, Symbion Science Park, Novo Nordisk A/S, Fruebjergvej 3, DK-2100 Copenhagen, Denmark

1. To investigate the mechanisms regulating the reuptake of secretory granule membranes following regulated exocytosis, we have monitored changes in cell capacitance in single pancreatic β-cells.

2. Membrane retrieval (endocytosis) occurred both in a continuous manner and in abrupt steps, corresponding to the simultaneous retrieval of 50–100 granules. The large endocytotic steps were associated with a conductance change of about 1 nS which we attribute to the formation of a fission pore with a pore radius of ~1 nm.

3. In some cells, we observed large amplitude capacitance fluctuations, suggesting that aggregates of granules are connected to the plasma membrane by a single pore and are subsequently retrieved as a single unit.

4. Endocytosis was evoked by elevation of cytosolic $[Ca^{2+}]_i$, but once initiated, a sustained increase in $[Ca^{2+}]_i$ was not required for endocytosis to continue.

5. The $[Ca^{2+}]_i$ dependence of exo- and endocytosis was studied by photorelease of Ca^{2+} from the 'caged' precursor Ca^{2+}–nitrophenyl-EGTA (Ca^{2+}–NP-EGTA). Both exo- and endocytosis were initiated at between 0·5 and 2 μM Ca_i^{2+}. The rate of endocytosis saturated above 2 μM Ca_i^{2+}, whereas exocytosis continued to increase up to 4 μM Ca_i^{2+}. The maximum rate of endocytosis was $<25\%$ of that of exocytosis.

6. Unlike exocytosis, endocytosis proceeded equally well in the presence or absence of Mg-ATP.

7. Our data indicate that in the pancreatic β-cell, exocytosis and endocytosis are regulated by different mechanisms.

Exocytosis involves the fusion of the secretory granule membrane with the plasma membrane. The granule membrane must subsequently be retrieved (endocytosis) in order to maintain a constant cell size and to recapture granular membrane components. In pancreatic β-cells, the first evidence for endocytosis of insulin secretory granules came from ultrastructural studies of horseradish peroxidase uptake into endocytotic vesicles (Orci, Malaisse-Lagae, Ravazzola & Amherdt, 1973). However, little information is available about the kinetics or the molecular mechanisms involved in the endocytosis of insulin granules.

Changes in cell capacitance occur when secretory granules are inserted into or removed from the plasma membrane (Neher & Marty, 1982) and have been used to monitor exo- and endocytosis in various cell types, including pancreatic β-cells (Gillis & Misler, 1992; Thomas, Wong, Lee & Almers, 1993; Thomas, Lee, Wong & Almers, 1994). This method can also provide information about the fission pore which forms during the course of the invagination and pinching off of the endocytosed membrane (Breckenridge & Almers, 1987; Rosenboom & Lindau, 1994). In this paper we describe the properties of endocytosis in mouse pancreatic β-cells, using the capacitance technique. We demonstrate that endocytosis is initiated by elevation of intracellular Ca^{2+}, as is the case in other neuroendocrine cells (Neher & Zucker, 1993; Heinemann, Chow, Neher &

Lena Eliasson and Peter Proks contributed equally to this work and should be considered as joint first authors.

§ To whom correspondence should be addressed.

Zucker, 1994; Thomas *et al.* 1994; Burgoyne, 1995), and that once endocytosis has been initiated, a sustained elevation of Ca^{2+} is not necessary for it to proceed. Finally, we show that endocytosis in the β-cell, unlike exocytosis, does not require Mg-ATP.

METHODS

Cell preparation

NMRI mice were killed by cervical dislocation and pancreatic islets isolated by collagenase digestion and dispersed into single β-cells by low-Ca^{2+} treatment (Ämmälä, Eliasson, Bokvist, Larsson, Ashcroft & Rorsman, 1993*b*). Cells were plated in plastic Petri dishes and maintained for up to 3 days in RPMI 1640 tissue culture medium supplemented with 10% fetal calf serum, 10 U ml^{-1} penicillin and 10 μg ml^{-1} streptomycin. Tissue culture chemicals were obtained from Life Technologies (Paisley, UK) or Northumbria Biologicals (Irvine, UK).

Recording methods

Patch pipettes were pulled from borosilicate glass capillaries, coated with Sylgard at their tips and fire polished immediately before use. They had resistances of 2–5 MΩ when filled with pipette solution. The access resistance during standard whole-cell recordings was typically <10 MΩ.

Whole-cell currents and changes in cell capacitance and conductance were recorded using an EPC-7 patch clamp amplifier (List Electronic, Darmstadt, Germany). Both the standard and perforated patch whole-cell configurations of the patch clamp method were used. The holding potential was set at −70 mV. Changes in cell capacitance and conductance were measured as previously described (Ämmälä *et al.* 1993*b*). Briefly, a 28 mV peak-to-peak 800 Hz sine wave was added to the holding potential and ten cycles averaged for each data point. The resulting current was analysed at two orthogonal phase angles with a resolution of 100 ms per point. The phase angle was determined empirically for each experiment by varying the G_{series} and C_{slow} knobs on the amplifier. Capacitance changes were evoked by infusion of Ca^{2+}-containing solutions (Augustine & Neher, 1992), by voltage clamp depolarizations (Ämmälä *et al.* 1993*b*) or by photoliberation of caged Ca^{2+} (Zucker, 1994; Bokvist, Eliasson, Ämmälä, Renström & Rorsman, 1995). Measurements were carried out using a Digidata or Labmaster AD converter (Axon Instruments, Foster City, CA, USA) with a 486 PC computer and in-house software written in Axobasic.

Solutions

The standard extracellular (bath) solution contained (mM): 140 NaCl, 5·6 KCl, 1·2 $MgCl_2$, 5–10 Hepes and 10–20 mM TEA (to block voltage-gated K^+ currents); adjusted to pH 7·4 with NaOH. The extracellular Ca^{2+} concentration was 2·6 mM except where otherwise indicated. For standard whole-cell recordings, the pipette was filled with (mM): 125 potassium glutamate, 1 $MgCl_2$, 3 Mg-ATP (unless otherwise indicated), 5 Hepes and a Ca^{2+}-EGTA buffer; adjusted to pH 7·15 with KOH. For the Ca^{2+} infusion experiments (Fig. 7), this comprised 1–10 mM EGTA and Ca^{2+} concentrations from 0 to 10 mM to produce free-Ca^{2+} concentrations between < 1 nM and 10 μM. When exocytosis was evoked by depolarization, the EGTA concentration was 50 μM and no Ca^{2+} was added. The Ca^{2+} concentrations were calculated using the binding constants of Martell & Smith (1971). In perforated patch experiments, the pipette solution contained (mM): 76 Cs_2SO_4, 10 KCl, 10 NaCl, 5 Hepes and 1 $MgCl_2$; adjusted to pH 7·4 with CsOH. Perforation was produced by inclusion of 0·24 mg ml^{-1} amphotericin B in the pipette solution (Rae, Cooper, Gates & Watsky, 1991). Perforation was considered adequate when the series conductance exceeded 40 nS. Forskolin (2–10 μM) was included in the extracellular solution in most experiments to increase the capacitance response (Ämmälä, Ashcroft & Rorsman, 1993*a*). Forskolin was dissolved in DMSO (final concentration < 0·1%). The bath was continuously perfused and all experiments were carried out at 30–34 °C.

Rapid elevation of the cytoplasmic Ca^{2+} concentration was produced by photoliberation of $Ca^{2+}$from Ca^{2+}–nitrophenyl-EGTA (Ca^{2+}–NP-EGTA; 2·4 mM Ca^{2+} and 3·8 mM NP-EGTA, Molecular Probes) (Ellis-Davies & Kaplan, 1994). Ca^{2+}–NP-EGTA was included in the pipette solution and the cell was dialysed for ~2 min prior to photorelease of Ca^{2+}. This should be sufficient for washout of endogenous ATP from the cell in experiments where the pipette solution lacked ATP. The washout of ATP in β-cells can be monitored as an increase in the ATP-activated K^+ current ($I_{K,ATP}$) (Rorsman & Trube, 1985) and rundown of this current suggests that ATP falls to < 1 μM within 2 min of cell dialysis (Ashcroft & Kakei, 1989). Photolysis was effected by a <3 ms flash of UV light using a flash apparatus (XF10, Hi-Tech Scientific, Salisbury, UK) as previously described (Bokvist *et al.* 1995).

Ca^{2+} measurements

$[Ca^{2+}]_i$ was estimated by dual-wavelength excitation spectrofluorimetry using fura-2 (Fig. 6) or the low-affinity Ca^{2+} indicator BTC (Iatridou, Foukaraki, Kuhn, Marcus, Haugland & Katerinopoulos, 1994; and see Fig. 8) as described elsewhere (Bokvist *et al.* 1995). For the fura-2 measurements, the cells were loaded with the ester form of the indicator (0·1 μM) in the culture medium for 20–25 min prior to the experiment, and cells with low fluorescence intensity were selected to minimize the effects of the Ca^{2+}-chelating action of the indicator. In Fig. 8, BTC was included in the pipette-filling solution (which dialyses into the cell) at a concentration of 40 μM.

Data analysis

The process of endocytosis is extremely variable in β-cells (see Results). We have confined our analysis of the rate of membrane retrieval to those cells in which endocytosis was continuous and could be fitted by an exponential time course: cells showing rapid endocytotic steps were excluded from this analysis. The conductance of the fission pore (G_p in Figs 10 and 11) was calculated as described by Breckenridge & Almers (1987). Capacitance and conductance points lying within 2 standard deviations of the noise level of the maximum capacitance and minimum conductance levels were excluded from this analysis.

Data are presented as means ± S.E.M. and statistical significances were calculated using Student's *t* test.

RESULTS

Endocytosis elicited by single depolarizations

Figure 1*A* shows the increase in cell capacitance evoked by a 500 ms depolarization from −70 to 0 mV in a standard whole-cell recording. The capacitance increase amounted to 150 fF, which corresponds to the release of seventy-five secretory granules since a single granule contributes about 2 fF (Ämmälä *et al.* 1993*b*). In 75% of the experiments using the standard whole-cell configuration (128/169 cells),

the cell capacitance remained constant or even increased following the initial exocytotic step elicited by the pulse.

When using the perforated patch whole-cell configuration (in which cell dialysis does not occur), the increase in cell capacitance evoked by the depolarization was typically transient and was followed by a return to the pre-stimulatory level (Fig. 1*B* and *C*). This decrease in capacitance may be interpreted as the retrieval of the previously secreted membrane, a process known as endocytosis. In contrast to standard whole-cell recordings, complete membrane retrieval was observed in 70% of perforated patch recordings (242/345 cells).

The rate of endocytosis was very variable, both between different cells and during membrane retrieval following a single depolarization. In many cases (Fig. 1*B*), the capacitance declined continuously with an endocytotic rate at least 30-fold slower than the mean rate of exocytosis observed during the preceding depolarization. Large step decreases in cell capacitance (> 20 fF) were also observed in about 30% of cells. Figure 1*C* illustrates a rapid endocytotic step of 200 fF. This would correspond to the simultaneous retrieval of one hundred vesicles or to the uptake of a single vesicle with a diameter of 2·5 μm, tenfold larger than that of the β-cell secretory granule, which has a diameter of 0·25 μm (Dean, 1973). In many cells, membrane retrieval involved a mixture of both abrupt and continuous endocytosis.

Rate of endocytosis

The time course of endocytosis was more easily observed following repetitive stimulation, when the exocytotic responses are large (Fig. 2*B* and *C*), than following a single depolarization (Fig. 2*A*). When exocytosis was enhanced, the amount of endocytosis correspondingly increased so that the capacitance usually returned to the pre-stimulatory level (Fig. 2*B* and *C*). Slow continuous endocytosis was observed in 50% (17/34) of cells. In the remaining cells, endocytosis consisted of a mixture of both continuous membrane retrieval and abrupt endocytotic steps (> 20 fF amplitude).

In most cases, continuous endocytosis could be fitted by a single exponential (Fig. 2*A*). In these experiments, the mean time constant for endocytosis (τ) following a single pulse was 76 ± 15 s ($n = 33$) and that following a train of ten pulses was 276 ± 112 s ($n = 12$). The corresponding mean amplitudes of endocytosis were 125 ± 23 and 408 ± 62 fF, respectively. In a few experiments, the capacitance decrease was best fitted (after some initial deviation) by a straight line (Fig. 2*B*) or by the sum of two exponentials (Fig. 2*C*).

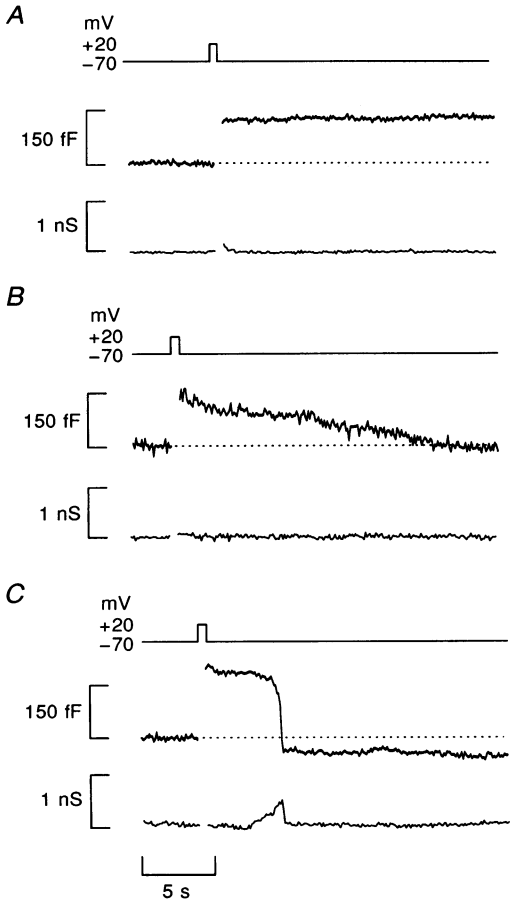

Figure 1

Capacitance changes produced by a 500 ms depolarization from −70 to 0 mV using the standard whole-cell recording configuration (*A*) and the perforated patch recording configuration (*B* and *C*). The voltage clamp depolarization is indicated above the records. The dashed line indicates the pre-stimulatory capacitance level. Note the presence of excess endocytosis in *C*.

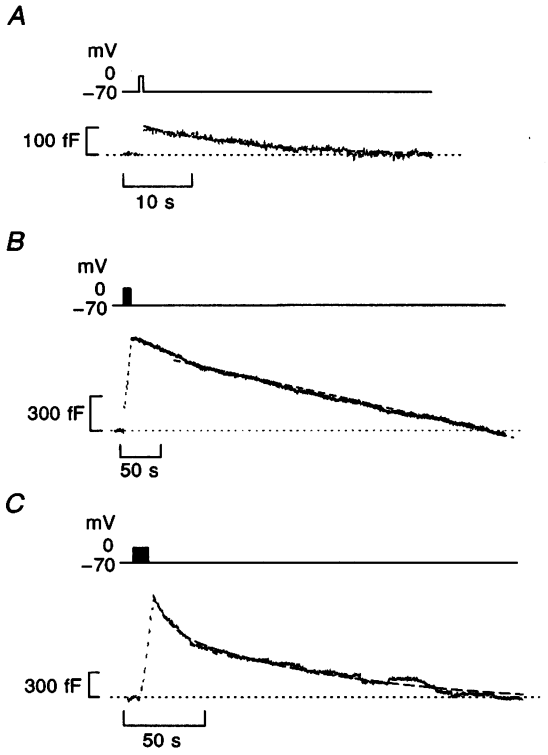

Figure 2

Examples of continuous endocytosis following a single 200 ms pulse (*A*) or a train of ten 200 ms pulses (frequency, 1 Hz) (*B* and *C*). Capacitance time courses were fitted by either a single exponential (*A*, $\tau = 12$ s), two exponentials (*C*, $\tau_1 = 10$ s, $\tau_2 = 119$ s) or a straight line (*B*, slope = 1·7 fF s^{-1}). The exponential or linear functions approximated to the observed data have been superimposed (dashed black curves) on the original data points (displayed in grey for clarity). Recordings were made from different β-cells using the perforated patch whole-cell configuration.

To compare the rate of endocytosis under different conditions, we have used the time constant determined from the experiments where the decline in cell capacitance could be fitted by a single exponential. Above 200 fF, there was no relationship between the magnitude of endocytosis and the time constant of endocytosis, but when endocytosis was smaller than 100 fF, the time constant of endocytosis increased with the extent of endocytosis (Fig. 3). Neither forskolin (to activate protein kinase A (PKA)) nor the phorbol ester, 4β-phorbol 12-myristate 13-acetate (PMA; to activate protein kinase C (PKC)), which both potentiate exocytosis (Ämmälä *et al.* 1993*a*, 1994), affected the rate of endocytosis, indicating that membrane retrieval is not accelerated by these kinases (data not shown).

Endocytosis is Ca^{2+} dependent

Figure 4*A* shows that reduction of the pulse duration from 500 ms (left) to 200 ms (right) decreased Ca^{2+} entry from 31 to 14 pC. Whereas the longer depolarization was followed by a rapid capacitance decrease to below the prestimulatory level (excess endocytosis; Thomas *et al.* 1994), there was no endocytosis following the second, shorter depolarization. This suggests that the rate and extent of endocytosis may depend on the amount of Ca^{2+} entry. To explore this possibility further, we investigated the capacitance changes elicited by depolarization in 2·6 and 20 mM extracellular Ca^{2+}. Elevation of extracellular Ca^{2+} increased the mean Ca^{2+} entry from 19 ± 2 pC ($n = 37$) to 33 ± 3 pC ($n = 13$) and dramatically accelerated the rate of endocytosis (Fig. 4*B* and *C*). Indeed, in some cells, elevation of external Ca^{2+} accelerated endocytosis to the extent that exocytosis was not discernible (see also Fig. 5*B*). The fast capacitance decay observed in 20 mM Ca^{2+} was not associated with any concomitant conductance changes, which suggests that it results from membrane retrieval and not a (Ca^{2+}-dependent) conductance change. The mean time constant of continuous endocytosis was 2·5 ± 1·4 s ($n = 6$) in 20 mM Ca^{2+} compared with 76 ± 15 s ($n = 33$) in 2·6 mM Ca^{2+}, and the mean

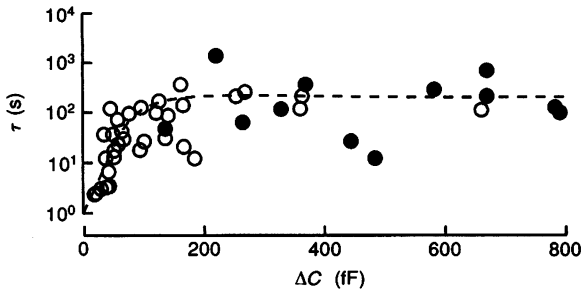

Figure 3

Time constant of endocytosis (τ) as a function of amount of retrieved capacitance (ΔC) elicited by single 500 ms depolarizations (○) or a train of ten 200 ms depolarizations (●). The dashed line is drawn by hand. Linear regression analysis of the data points in the interval up to 100 fF yielded a slope of 0·7 s fF^{-1} ($r = 0{\cdot}45$; $P \approx 0{\cdot}05$)

decrease in cell capacitance was 115 ± 29 and 125 ± 23 fF, respectively. The higher rate of membrane retrieval seen at elevated Ca^{2+} is therefore not a consequence of a smaller endocytotic response (Fig. 3).

Following elevation of $[Ca^{2+}]_o$ to 20 mM, more than 50% of single pulses were followed by endocytotic steps (Fig. 5*A*), compared with 27% of single depolarizations in 2·6 mM Ca^{2+}. Increasing extracellular Ca^{2+} also increased the amplitude of the endocytotic steps; from 33 ± 7 fF ($n = 62$) in 2·6 mM Ca^{2+} to 79 ± 11 fF ($n = 33$) at 20 mM Ca^{2+}. Excess endocytosis was also more common (Fig. 5*A* and *B*). Although endocytosis rarely occurred in standard whole-cell recordings with 2·6 mM extracellular Ca^{2+}, membrane retrieval was observed in four out of seven cells when Ca^{2+} was raised to 20 mM (Fig. 5*C*).

These observations suggest that endocytosis in the β-cell, as in other neuroendocrine cells, is dependent on an elevation of intracellular Ca^{2+}. We therefore investigated the relationship between endocytosis and the cytoplasmic $[Ca^{2+}]_i$. Figure 6 shows simultaneous recordings of cell capacitance and $[Ca^{2+}]_i$ elicited by a train of depolarizations. During stimulation, $[Ca^{2+}]_i$ rose to ~3 μM and there was an associated increase

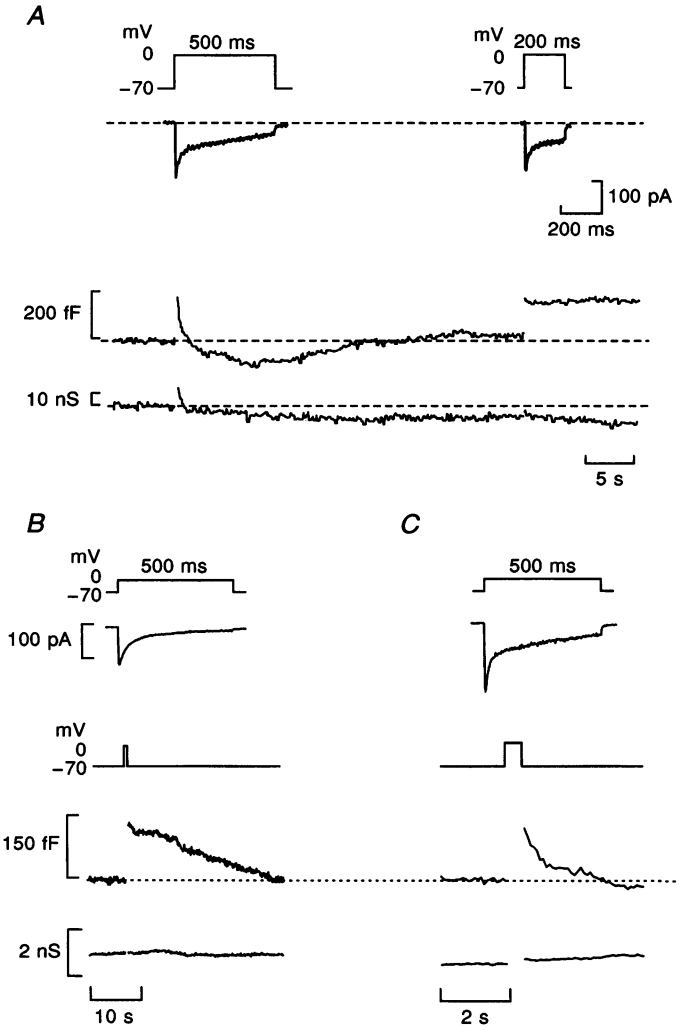

Figure 4

A, Ca^{2+} currents (top), capacitance (middle) and conductance changes (bottom) produced by a 500 ms and a consecutive 200 ms depolarization from −70 to 0 mV in 2·6 mM extracellular Ca^{2+}. The prestimulatory capacitance level is indicated by the dashed line. The voltage clamp depolarization is indicated above the record. Note that the time scale is different for the current and capacitance traces. Recordings were made using the perforated patch whole-cell configuration. *B* and *C*, Ca^{2+} currents (top), capacitance (middle) and conductance changes (bottom) produced by a 500 ms depolarization from −70 to 0 mV in 2·6 mM (*B*) or 20 mM (*C*) extracellular Ca^{2+}. The prestimulatory capacitance level is indicated by the dashed line. The voltage clamp depolarization is indicated above the records, which were obtained from two different cells of the same preparation.

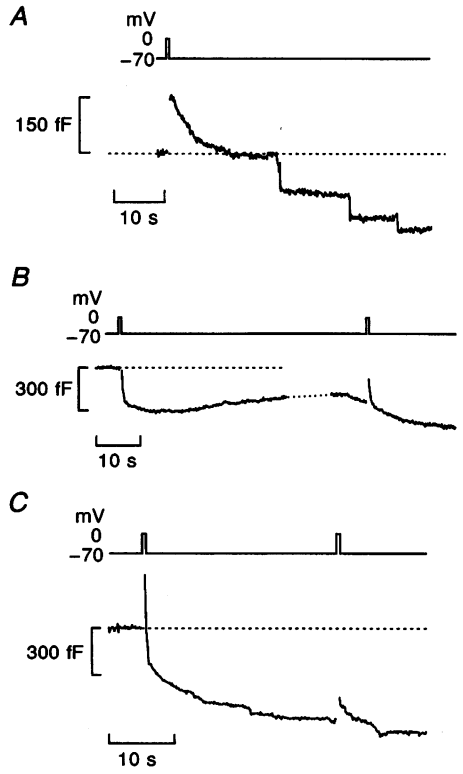

Figure 5. Endocytosis in the presence of 20 mM extracellular Ca^{2+}

A, examples of endocytotic steps evoked by a single 500 ms depolarization. *B*, continuous endocytosis evoked by two consecutive depolarizations. Recordings in *A* and *B* were obtained using the perforated patch whole-cell configuration. *C*, exo- and endocytotic responses elicited by two consecutive depolarizations using the standard whole-cell configuration. The dashed lines indicate the prestimulatory capacitance level.

in cell capacitance. Following the cessation of stimulation, $[Ca^{2+}]$ rapidly (< 5 s) fell to below 0·5 μM whereas endocytosis continued for several minutes. There was no change in $[Ca^{2+}]_i$ associated with the endocytotic steps. On average, the $[Ca^{2+}]_i$ transient had fallen by 81 ± 9% ($n = 8$) by the time 10% of the exocytosed membrane had been retrieved. The mean time constant for the decay of the $[Ca^{2+}]_i$ transient was 3·0 ± 0·3 s ($n = 8$), much faster than that of endocytosis (~80 s, see above). These data therefore suggest that endocytosis is initiated by an initial transient increase in $[Ca^{2+}]_i$, but that membrane retrieval can then proceed at $[Ca^{2+}]_i < 200$ nM.

As shown in Fig. 6 (inset), a delay between the cessation of stimulation and the onset of endocytosis was sometimes observed. This delay was more common following intense stimulation, being observed in 52% of experiments with repetitive stimulation as compared with 14% of experiments with single pulses. In these cells, the mean latency was unaffected by the stimulus intensity: 7 ± 2 s ($n = 5$) and 7 ± 1 s ($n = 10$) for single pulses and trains, respectively. A similar delay has been reported for synaptic terminals (von Gersdorff & Matthews, 1994) and attributed to inhibition of endocytosis by high $[Ca^{2+}]_i$. An alternative explanation is that endocytosis is transiently masked by continuing exocytosis.

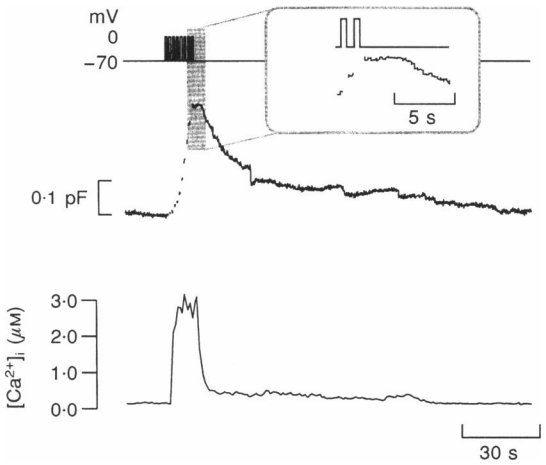

Figure 6

Changes in cell capacitance (middle) and intracellular Ca^{2+} (below) elicited by a train of 11 depolarizations from −70 to 0 mV (top). Inset, expanded section of the capacitance trace showing the delay between the cessation of stimulation and the onset of endocytosis.

Endocytosis is independent of intracellular ATP

Infusion of the β-cell with different Ca^{2+} concentrations resulted in a continuous increase in cell capacitance, the rate of which increased as Ca^{2+} was elevated. Endocytosis was not apparent until Ca^{2+} was increased to 10 μM, when a very pronounced membrane uptake often occurred (Fig. 7*A*). In many cells endocytosis ceased before all the secreted membrane had been recovered, which may suggest that membrane uptake requires a diffusible cytosolic component which is washed out of the cell.

We investigated whether endocytosis requires Mg-ATP by repeating these experiments in the absence of ATP (Fig. 7*B* and *C*). In most cases (9/12 cells), the increase in cell capacitance elicited by 2 or 10 μM Ca^{2+} in the absence of ATP was followed by a capacitance decrease. The maximum rates of endocytosis observed at 2 and 10 μM Ca_i^{2+} averaged 47 ± 23 fF s^{-1} ($n = 4$) and 111 ± 24 fF s^{-1} ($n = 8$), respectively. Endocytosis was not observed at $[Ca^{2+}]_i$ below 2 μM: this suggests the threshold $[Ca^{2+}]_i$ for initiation of endocytosis lies between 0·5 and 2 μM. Like endocytosis elicited by depolarization in intact cells, membrane retrieval consisted of both a slow and continuous decrease in capacitance (Fig. 7*A* and *B*) and large endocytotic steps (Fig. 7*C*). These data indicate that ATP is not required for endocytosis in the β-cell and confirm that endocytosis is a Ca^{2+}-dependent process. To investigate the relationship between $[Ca^{2+}]_i$, ATP, exocytosis and endocytosis in greater detail, we next elevated $[Ca^{2+}]_i$ by photorelease from Ca^{2+}–NP-EGTA ('caged Ca^{2+}') in the presence (Fig. 8*A*) and absence of Mg-ATP (Fig. 8*B*). In the presence of 3 mM ATP, the first flash elevated $[Ca^{2+}]_i$ to 3 μM after which it gradually declined to 1 μM. This was parallelled by an immediate capacitance step of 500 fF followed by a further gradual increase of 1 pF. A second flash, which increased $[Ca^{2+}]_i$ to >3·5 μM, produced a transient increase (100 fF) in cell capacitance and a subsequent rapid decrease in cell capacitance of 0·5 pF. When $[Ca^{2+}]_i$ was elevated in the absence of Mg-ATP, however, exocytosis was suppressed and the first flash now transiently reduced the cell capacitance by ~60 fF and the second flash was without effect on endocytosis.

The mean results are summarized in Fig. 8*C*. Although the increase in $[Ca^{2+}]_i$ was somewhat larger in the absence of Mg-ATP (possibly reflecting inhibition of ATP-driven Ca^{2+}-extrusion pathways), exocytosis was reduced by ~90%. Endocytosis was little affected by the omission of Mg-ATP.

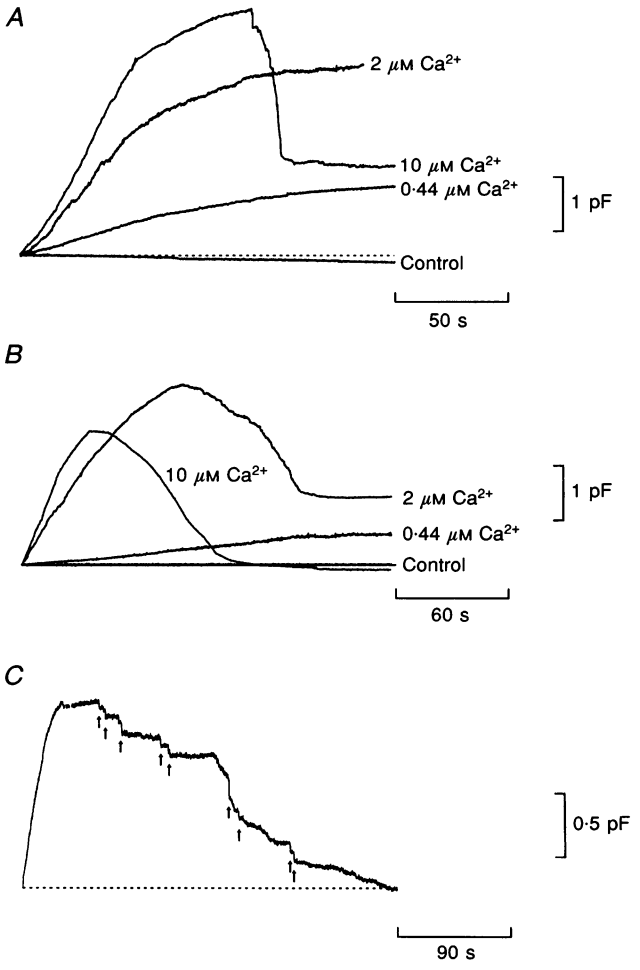

Figure 7

Capacitance changes produced by intracellular dialysis with a solution containing various Ca^{2+} concentrations (indicated to the right of the capacitance traces; control: <10 nM) in the presence (*A*) or absence (*B*) of 3 mM Mg-ATP. The standard whole-cell configuration was established <20 s before the recordings begin. The data come from different cells. *C*, capacitance change produced by intracellular dialysis with a solution containing 2 μM Ca^{2+} and no ATP. In *A* and *C*, the initial capacitance level is indicated by the dashed line. The arrows indicate the large endocytotic steps.

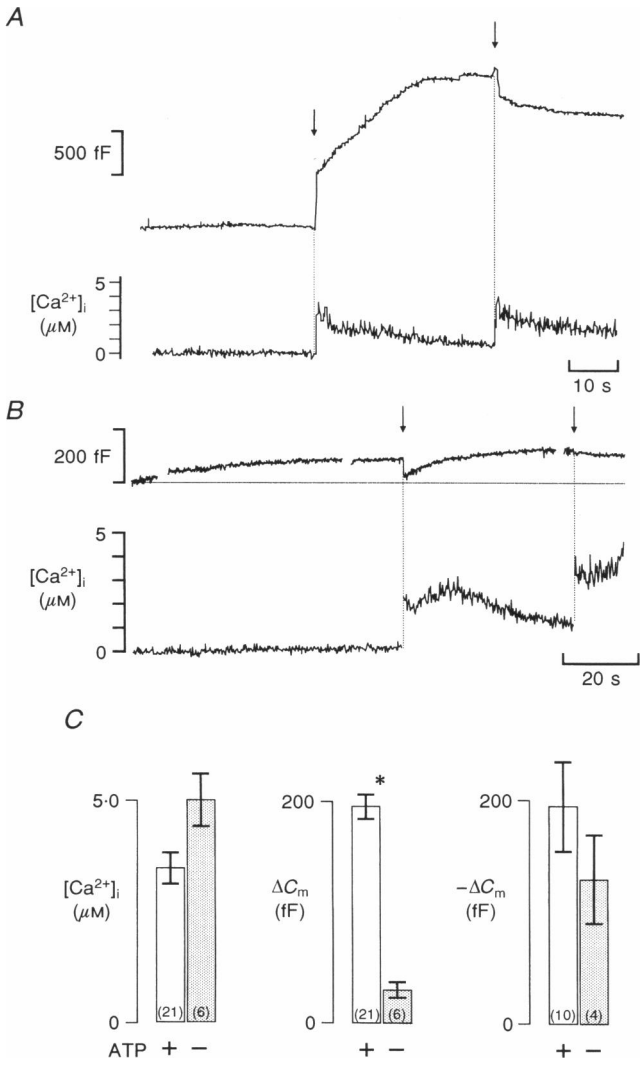

Figure 8

Changes in cell capacitance (above) and intracellular Ca^{2+} (below) elicited by photorelease (arrows and vertical dotted lines) of Ca^{2+} from the caged precursor Ca^{2+}–NP-EGTA in the presence (*A*) and absence (*B*) of Mg-ATP. In *B*, the dotted horizontal line indicates the capacitance level observed shortly after establishing the whole-cell configuration. Note the spontaneous increase in cell capacitance. *C*, mean increase in $[Ca^{2+}]_i$ (left), mean capacitance increase (middle) and mean capacitance decrease (right) elicited by photorelease of Ca^{2+} in the presence (□) and absence (▨) of Mg-ATP. Only the responses to the first flash in each experiment have been included. Data are mean values ± S.E.M. of the number of *n* experiments (indicated in parentheses). * $P < 0{\cdot}001$.

The observation that endocytosis is larger than exocytosis in the absence of Mg-ATP may be attributed to the retrieval of additional membrane which was inserted shortly after establishment of the whole-cell configuration before cell dialysis was complete. The initial increase in cell capacitance seen in whole-cell recordings from cells dialysed with 0 Mg-ATP may be attributed to the presence of endogenous ATP, which sustains exocytosis for a brief period before it is washed out of the cell. The time course of this washout may be estimated from the associated increase in the $I_{K,ATP}$ and is usually complete within < 2 min.

Collectively these data suggest that exocytosis, but not endocytosis, is dependent on the presence of intracellular Mg-ATP.

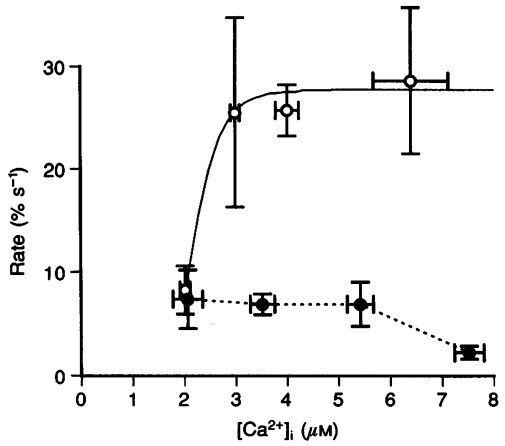

Figure 9

Ca^{2+} dependence of exocytosis (○) and endocytosis (●) evoked by photorelease of Ca^{2+} from Ca^{2+}–NP-EGTA. The observed rates of exo- and endocytosis (in fF s^{-1}) were normalized to the respective cell capacitance and expressed as the percentage increase in cell capacitance per second. Thus, an exocytotic rate of 500 fF s^{-1} in a cell with a capacitance of 5 pF corresponds to a percentage rate of 10 % s^{-1}. Mean values ± S.E.M. of 3–8 experiments.

$[Ca^{2+}]_i$ dependence of exo- and endocytosis

The $[Ca^{2+}]_i$ dependence of exocytosis and endocytosis derived from the experiments using caged Ca^{2+} is summarized in Fig. 9. The rate of exocytosis was dependent on $[Ca^{2+}]_i$, with half-maximal stimulation (EC_{50}) being observed at 2·2 μM close to that reported previously (1·4 μM; Bokvist *et al.* 1995) and observed for Ca^{2+} infusion (P. Proks, L. Eliasson, Ö. Ammälä, P. Rorsman & F. M. Ashcroft, unpublished data). In contrast, the rate of endocytosis was not detectably influenced by variations of $[Ca^{2+}]_i$ in the range between 2 and 5·5 μM and at higher concentrations there was even a tendency towards inhibition. At ~2 μM Ca_i^{2+}, exocytosis and endocytosis proceeded at comparable rates. It could be argued that the saturation of the relationship between $[Ca^{2+}]_i$ and endocytosis above 2 μM Ca_i^{2+} results from membrane retrieval being masked by concomitant exocytosis. This is unlikely to be the case, however, as a similar saturation was also observed in the absence of Mg-ATP when there was no or little exocytosis.

Properties of the fission pore predicted from the conductance changes associated with large endocytotic steps

As already discussed, endocytotic steps similar to those found in pituitary nerve terminals (Rosenboom & Lindau, 1994) were observed in ~30% of the cells (Fig. 1). When such large endocytotic steps were observed they were often associated with a transient increase in cell conductance. These conductance changes can be used to estimate the properties of the fission pore (Fig. 10). We have confined our analysis of the endocytotic steps to those which were associated with distinct changes in cell conductance lasting >300 ms (i.e. three sample points). The mean capacitance increase in these experiments amounted to 142 ± 16 fF ($n = 11$) and the mean capacitance decrease was 140 ± 19 fF ($n = 11$): in six of these experiments, the amount of membrane retrieved during the abrupt step was greater than that inserted by exocytosis. The abrupt endocytotic steps occurred on average 12 ± 4 s ($n = 11$) after the end of the pulse and the mean lifetime of the fission pore was 0·8 ± 0·2 s ($n = 11$). The lifetime of the

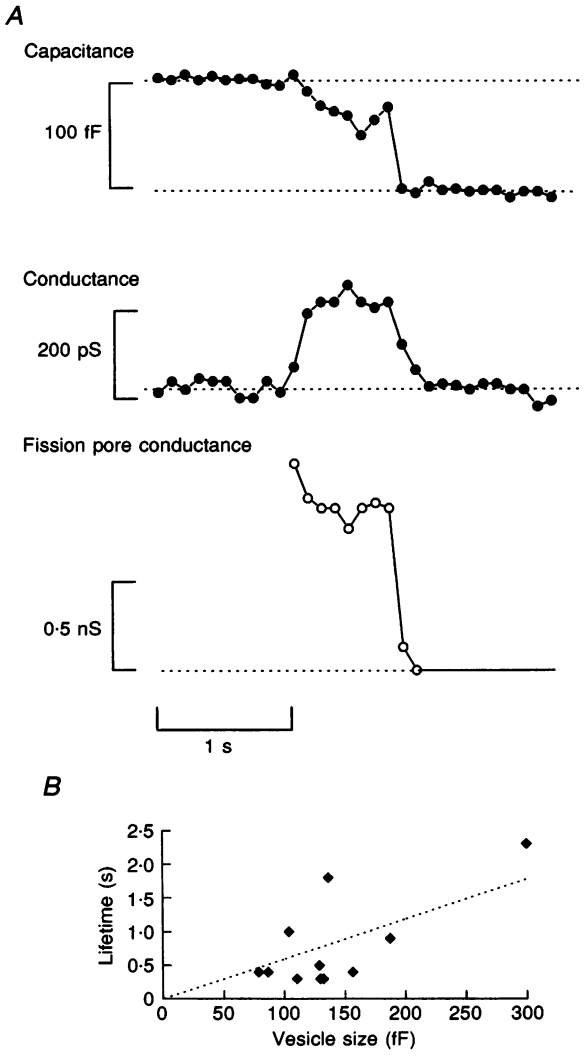

Figure 10

A, capacitance, conductance and calculated fission pore conductance changes during an endocytotic step. *B*, the relationship between the lifetime of the fission pore and the vesicle size (as indicated by the amplitude of endocytotic step). The dotted line is the best linear fit to the data and has a slope of 0·6 ms fF^{-1} ($r = 0·73$, $P < 0·01$).

endocytotic particle increased slightly with its size, the slope of the relationship being 0·6 ± 0·1 ms fF^{-1} (Fig. 10*B*). The conductance of the fission pore can be calculated from the measured capacitance and conductance changes, as described previously by Breckenridge & Almers (1987) and Rosenboom & Lindau (1994). In five cells, the fission pore exhibited a semi-stable state before finally closing (Fig. 10*A*) with an estimated mean conductance of 1·4 ± 0·3 nS.

Capacitance flickers suggest multivesicular membrane retrieval

In less than 1% of the experiments (12 out of 345 cells) we observed endocytotic capacitance flickers similar to those reported for exocytosis in mast cells (Breckenridge & Almers, 1987) and chromaffin cells (Artalejo, Henley, McNiven & Palfrey, 1995). Figure 11*A* shows one such example. The amplitude of the capacitance flickers would be equivalent to the simultaneous uptake and retrieval of around twenty-five secretory granules or a single vesicle with diameter of 1·2 μm. The capacitance flickers always began and ended with membrane uptake, suggesting that the process involves endocytosis. We propose that the endocytotic flickers may result from transient changes in the size of the fission pore (Fig. 11*C*). Thus, when the fission pore is small and has a high access resistance, the vesicle capacitance will no longer be detectable, but when the pore size increases again and the access resistance is reduced, the granular capacitance will once more be measurable.

In some cases (5 out of 12) it was possible to resolve conductance changes associated with the fission pore. This enabled us to calculate the conductance of the fission pore itself (G_p). An example of the fission pore conductance changes associated with the capacitance flickers is shown

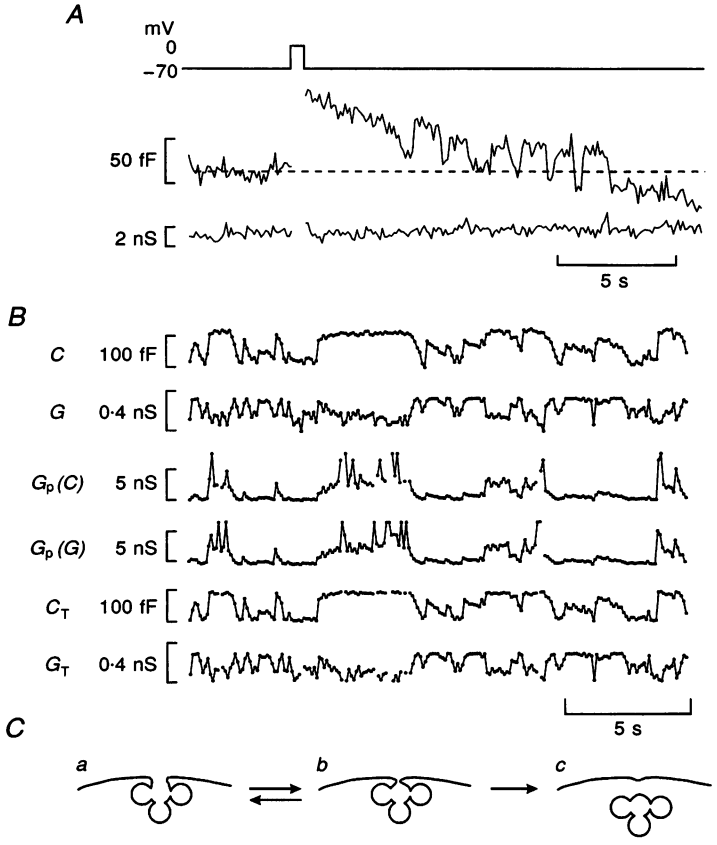

Figure 11

A, capacitance (middle) and conductance (bottom) changes produced by a 500 ms depolarization from −70 to 0 mV (top) using the perforated patch recording configuration. The dashed line indicates the pre-stimulatory capacitance level. *B*, capacitance flickers following a 200 ms depolarization from −70 to 0 mV in another cell, displayed on a fast time base. The data points are indicated by dots (sample rate, 10 Hz). *C*, measured capacitance; *G*, measured conductance trace; $G_p(C)$, conductance of the fission pore calculated from the measured capacitance; $G_p(G)$, conductance of the fission pore calculated from the measured conductance; C_T, capacitance calculated from $G_p(G)$; G_T, conductance trace calculated from $G_p(C)$. *C*, model explaining the origin of the capacitance flickers: *a*, fission pore formed but open, no change in cell capacitance; *b*, fission pore (reversibly) closes, resulting in a (transient) decrease in cell capacitance; *c*, fission pore closes (irreversibly) and vesicle dissociates from the plasma membrane resulting in a permanent decrease in cell capacitance.

in Fig. 11*B*. The lower two traces show the theoretical capacitance (C_T) and conductance (G_T) changes predicted from the conductance of the fission pore, calculated from the measured conductance or capacitance changes, respectively. The close agreement of these calculated traces (C_T, G_T) with the measured changes (C, G) indicates that the latter arise entirely from changes in the conductance of the fission pore. The conductance of the fission pore (G_p) shows semi-stable states in the nanosiemens range, similar to those found for the fusion pore of mast cell secretory granules (Curran, Cohen, Chandler, Munson & Zimmerberg, 1993). The average value of the lower stable level was $2 \pm 0{\cdot}2$ nS ($n = 5$) when measured for capacitance steps >50 fF. This is comparable with that found for the single endocytotic steps (see above). It is clear from the calculated fission pore conductance that the 'closing' event takes several sample points whereas the 'opening' event occurs within a single sample point (Fig. 11*B*). Since each sample point is 100 ms, this suggests that the 'closing' of the fission pore requires up to 500 ms while the 'opening' takes place within 100 ms. Thus, the closing of the fission pore is not a rapid event analogous to the gating of an ion channel and the pore may be better explained in terms of a lipidic fusion pore (cf. Nanavarti, Markin, Oberhauser & Fernandez, 1992).

DISCUSSION

Endocytosis is Ca^{2+} dependent

Our data indicate that the primary factor regulating the rate of endocytosis is the cytoplasmic Ca^{2+} concentration. Thus endocytosis can be triggered by Ca^{2+} influx through voltage-dependent Ca^{2+} channels, by Ca^{2+} release from internal stores (Rorsman, Bokvist, Ämmälä, Eliasson & Gäbel, 1994), by infusion of high Ca^{2+} concentrations or by Ca^{2+} released from a caged precursor. Our results are in accordance with earlier reports that endocytosis can be triggered by high (>10 μM) Ca^{2+} concentrations in melanotrophs and chromaffin cells (Neher & Zucker, 1993; Thomas *et al.* 1994; Heinemann *et al.* 1994; Burgoyne, 1995).

In the β-cell, the threshold Ca^{2+} concentration for endocytosis in standard whole-cell recordings lies somewhere between 0·5 and 2 μM, irrespective of whether exocytosis is elicited by infusion with high Ca^{2+} buffers (Fig. 7) or by photorelease of Ca^{2+} from a caged precursor (Fig. 9). This $[Ca^{2+}]_i$ threshold is similar to that of exocytosis. The rates of both exo- and endocytosis are maximal above 4 μM Ca_i^{2+} but the rate of exocytosis is more than 3-fold faster than that of membrane retrieval. Since step increases in cell capacitance are observed in response to depolarization, our data suggest that exocytosis evoked by depolarization is associated with $[Ca^{2+}]_i$ at which the rate of exocytosis exceeds that of endocytosis (i.e. >2 μM).

Endocytosis continues for a considerable period after $[Ca^{2+}]_i$ has declined to its prestimulatory level (Fig. 6). It therefore appears that Ca^{2+}serves a priming function and is only required to initiate endocytosis. Once initiated, endocytosis proceeds in the absence of Ca^{2+}.

Endocytosis is ATP-independent

In contrast to exocytosis, endocytosis does not appear to require ATP. The 90% inhibition of exocytosis we observed when $[Ca^{2+}]_i$ is rapidly elevated in the absence of Mg-ATP is in good agreement with the 89% inhibition of Ca^{2+}-induced insulin secretion reported in permeabilized insulin-secreting cells (Regazzi *et al.* 1995). In permeabilized chromaffin cells, ATP is required for the priming of granules for release (Bittner & Holz, 1992), but primed granules may be released by Ca^{2+} elevation in the absence of Mg-ATP (Thomas *et al.* 1993; Parsons, Coorsen, Horstmann & Almers, 1995). The extreme ATP dependence of exocytosis we observe in β-cells suggests that the pool of 'primed granules' is smaller in the β-cell than in other neuroendocrine cells.

No effects of phosphorylation by PKA or by PKC were observed on endocytosis although activation of both these kinases potentiates exocytosis (Ämmälä *et al.* 1993*a*, 1994). This leads us to conclude that the mechanisms that regulate endocytosis are different from those that control exocytosis. In particular, whereas the effects of Ca^{2+} on exocytosis involve the activation of Ca^{2+}–calmodulin-dependent protein kinase II (CaMkII) (Ämmälä *et al.* 1993*b*), the fact that Ba^{2+}, which does not bind to calmodulin, is able to support endocytosis (Proks & Ashcroft, 1995), and the lack of requirement of ATP, indicate that CaMkII is not involved in membrane recycling. The ability of Ba^{2+} to support endocytosis also precludes the involvement of other calmodulin-dependent enzymes such as the protein phosphatase calcineurin. This is supported by the lack of effect of deltamethrin (0·1 μM) on endocytosis, an inhibitor of calcineurin (data not shown). In addition, since endocytosis does not require ATP it is unlikely that phosphorylation is involved in membrane retrieval.

Rapid loss of endocytosis in standard whole-cell recordings

Endocytosis is preserved in intact β-cells but is rapidly lost in standard whole-cell recordings. One explanation for the latter effect is that it results from the washout of a small soluble cytosolic factor. However, since endocytosis is lost within 10–20 s of the establishment of the whole-cell configuration, i.e. the minimum time between the establishment of the whole-cell configuration and the start of the capacitance measurements, it seems unlikely that washout is the only factor determining the loss of endocytosis (see also Parsons, Lenzi, Almers & Roberts, 1994). An alternative possibility is that wash-in of some low molecular weight substance from the pipette solution inhibits endocytosis. For example, EGTA may suppress endocytosis by chelating Ca^{2+}: with a typical access resistance of 5 MΩ, we estimate that EGTA reaches 70% of the pipette concentration within 10–30 s (Pusch & Neher, 1988). Because of its slow Ca^{2+}-binding kinetics, low

concentrations of EGTA may be expected to have only a small effect on exocytosis, which is controlled by the large and rapid $[Ca^{2+}]_i$ transients just beneath the membrane, but to have a more pronounced effect on processes which take place further away from the point of Ca^{2+} entry. This may explain why depolarization-evoked endocytosis is suppressed in standard whole-cell recordings, yet membrane retrieval can be elicited in dialysed cells when $[Ca^{2+}]_i$ is increased sufficiently (for example, by dialysis with Ca^{2+}-EGTA buffers, photorelease of 'caged' Ca^{2+} or Ca^{2+} mobilization induced by inositol 1,4,5 trisphosphate (IP_3)).

Vacuolar *versus* vesicular endocytosis

In some cells we observed stepwise decreases in cell capacitance which were far larger than those reported for single endocytotic events in β-cells (mean, 2 fF: Ämmälä *et al.* 1993*b*). These were more commonly elicited by high-intensity stimulation (trains of depolarizations or high Ca^{2+} concentrations; Figs 5 and 6). Similar findings have been reported in pituitary nerve terminals (Thomas *et al.* 1994; Rosenboom & Lindau, 1994). These large capacitance decreases (as much as 100 fF) could either represent the simultaneous endocytosis of many vesicles or the retrieval of a single large vesicle. We have considered three possibilities. Firstly, as cell capacitance is only calculated every 100 ms, it is possible that the large steps we observe do not constitute a single instantaneous event, but rather the sum of many small events which take place within this time period; however, the observation that large capacitance flickers can occur (Fig. 11) makes this unlikely. Secondly, the membrane from many vesicles incorporated into the plasma membrane may be endocytosed as a single unit. As the membrane between the granules would also be retrieved, this hypothesis would account for excess endocytosis seen under some experimental conditions (Figs 1, 4 and 5). Thirdly, large endocytotic steps might occur following multivesicular (compound) release, as suggested in mast cells (Alvarez de Toledo, Fernandez-Charon & Fernandez, 1993). Multivesicular release has been documented previously in endocrine cells, including pancreatic β-cells, by electron microscopy (Orci & Malaisse, 1980; Fujita, Kurikara & Miyagawa, 1983). The capacitance flickers observed in Fig. 11 are most easily explained by this possibility since it seems very unlikely that exactly the same number of individual vesicles undergo fusion and fission several times in succession.

The large endocytotic steps were often associated with a transient increase in the cell conductance. We attribute this to the formation of a fission pore, analogous to the fusion pore produced on exocytosis. The calculated conductance of the fission pore was in the range, 1–5 nS, which is similar to the fusion pore of giant secretory granules in mast cells (Curran *et al.* 1993). Assuming a single bilayer 4 nm thick and a solution resistivity of 100 Ω cm^{-1} (Nanavarti *et al.* 1992), the corresponding pore radius ranges between 1 and 3 nm or about 1–2% of the granule diameter (Dean, 1973). Vacuolar endocytosis with similar properties has been described in pituitary nerve terminals (Rosenboom & Lindau, 1994). The random oscillations in the size of the fission pore conductance that we observed suggest that the pore dilates and constricts in a fluctuating manner similar to that found for the fusion pore (Curran *et al.* 1993) and argues that the pore is lipidic in nature rather than proteinaceous.

The relationship between exocytosis and endocytosis

The fact that in most experiments the cell capacitance returned to its prestimulatory level indicates that the amount of membrane retrieved matched that previously secreted. This implies that the β-cell has a means of recognizing the amount of membrane exocytosed. This is most easily explained by assuming that the cell simply removes the secreted (granular) membrane. In some experiments, however, the amount of membrane endocytosed exceeded that inserted by exocytosis ('excess endocytosis').

The mechanism of endocytosis we observe is not clear but the magnitude of the endocytotic steps is too large to be explained by uptake of clathrin-coated vesicles, which are only around 0·1 μm in diameter (as compared with a calculated 1·2 μm), and thus some other mechanism of membrane retrieval must take place. It remains to be determined whether the mechanism regulating the uptake of the large vesicles is the same as that which controls the uptake of small vesicles.

Alvarez de Toledo, G., Fernandez-Charon, R. & Fernandez, J. M. (1993). Release of secretory products during transient vesicle fusion. *Nature* **363**, 554–558.

Ämmälä, C., Ashcroft, F. M. & Rorsman, P. (1993*a*). Calcium-independent potentiation of insulin release by cyclic AMP in single β-cells. *Nature* **363**, 356–358.

Ämmälä, C., Eliasson, L., Bokvist, K., Berggren, P.-O., Honkanen, R. E., Sjöholm, Å. & Rorsman, P. (1994). Activation of protein kinases and inhibition of protein phosphatases play a central role in the regulation of exocytosis in mouse pancreatic β-cells. *Proceedings of the National Academy of Sciences of the USA* **91**, 4343–4347.

Ämmälä, C., Eliasson, L., Bokvist, K., Larsson, O., Ashcroft, F. M. & Rorsman, P. (1993*b*). Exocytosis elicited by action potentials and voltage clamp calcium currents in individual pancreatic B-cells. *Journal of Physiology* **472**, 665–688.

Artalejo, C. R., Henley, J. R., McNiven, M. A. & Palfrey, C. H. (1995). Rapid endocytosis coupled to exocytosis in adrenal chromaffin cells involves Ca^{2+}, GTP and dynamin but not clathrin. *Proceedings of the National Academy of Sciences of the USA* **92**, 8328–8332.

Ashcroft, F. M. & Kakei, M. (1989). ATP-sensitive K^+-channels in rat pancreatic β-cells: modulation by ATP and Mg^{2+} ions. *Journal of Physiology* **416**, 349–367.

Augustine, G. J. & Neher, E. (1992). Calcium requirement for secretion in bovine chromaffin cells. *Journal of Physiology* **450**, 247–271.

BITTNER, M. A. & HOLZ, R. W. (1992). Kinetic analysis of secretion from permeabilized adrenal chromaffin cells reveals distinct components. *Journal of Biological Chemistry* **267**, 16219–16225

BOKVIST, K., ELIASSON, L., ÄMMÄLÄ, C., RENSTRÖM, E. & RORSMAN, P. (1995). Co-localization of L-type Ca^{2+}-channels and insulin containing secretory granules and its significance for the initiation of exocytosis in mouse pancreatic B-cells. *EMBO Journal* **14**, 50–57.

BRECKENRIDGE, L. J. & ALMERS, W. (1987). Currents through the fusion pore that forms during exocytosis of a secretory vesicle. *Nature* **328**, 814–817.

BURGOYNE, R. D. (1995). Fast exocytosis and endocytosis triggered by depolarization in single adrenal chromaffin cells before rapid Ca^{2+} current run-down. *Pflügers Archiv* **430**, 213–219.

CURRAN, M. J., COHEN, F. S., CHANDLER, D. E., MUNSON, P. J. & ZIMMERBERG, J. (1993). Exocytotic fusion pores exhibit semi-stable states. *Journal of Membrane Biology* **133**, 61–75.

DEAN, P. M. (1973). Ultrastructual morphometry of the pancreatic β-cell. *Diabetologia* **9**, 115–119.

ELLIS-DAVIES, G. C. R. & KAPLAN, J. H. (1994). Nitrophenyl-EGTA, a photolabile chelator that selectively binds Ca^{2+} with high affinity and releases it quickly upon photolysis. *Proceedings of the National Academy of Sciences of the USA* **91**, 187–191.

FUJITA, H., KURIKARA, H. & MIYAGAWA, J. (1983). Ultrastructual aspects of the effect of calcium ionphore A23187 on incubated anterior pituitary cells of rats. *Cell and Tissue Research* **229**, 129–136.

GILLIS, K. D. & MISLER, S. (1992). Single cell assay of exocytosis from pancreatic islet β-cells. *Pflügers Archiv* **420**, 121–123.

HEINEMANN, C., CHOW, R. H., NEHER, E. & ZUCKER, R. S. (1994). Kinetics of the secretory response in bovine chromaffin cells following flash photolysis of caged Ca^{2+}. *Biophysical Journal* **67**, 2546–2557.

IATRIDOU, H., FOUKARAKI, E., KUHN, M. A., MARCUS, E. M., HAUGLAND, R. P. & KATERINOPOULOS, H. E. (1994). The development of a new family of intracellular Ca^{2+}-probes. *Cell Calcium* **15**, 190–198.

MARTELL, A. E. & SMITH, R. M. (1971). *Critical Stability Constants*, vol. 1, *Amino Acids* and vol. 2, *Amines*. Plenum Press, New York.

NANAVARTI, C., MARKIN, V. S., OBERHAUSER, A. F. & FERNANDEZ, J. M. (1992). The exocytotic fusion pore modeled as a lipidic pore. *Biophysical Journal* **63**, 1118–1132.

NEHER, E. & MARTY, A. (1982). Discrete changes of cell membrane capacitance observed under conditions of enhanced secretion in bovine adrenal chromaffin cells. *Proceedings of the National Academy of Sciences of the USA* **79**, 6712–6716.

NEHER, E. & ZUCKER, R. S. (1993). Multiple calcium-dependent processes related to secretion in bovine chromaffin cells. *Neuron* **10**, 21–30.

ORCI, L. & MALAISSE, W. (1980). Hypothesis: single and chain release of insulin secretory granules is related to anionic transport at exocytotic sites. *Diabetes* **29**, 943–944.

ORCI, L., MALAISSE-LAGAE, F., RAVAZZOLA, M. & AMHERDT, M. (1973). Exocytosis–endocytosis coupling in the pancreatic beta cell. *Science* **181**, 561–562.

PARSONS, T. D., COORSEN, J. R., HORSTMANN, H. & ALMERS, W. (1995). Docked granules, the exocytotic burst and the need for ATP hydrolysis in endocrine cells. *Neuron* **15**, 1085–1096.

PARSONS, T. D., LENZI, D., ALMERS, W. & ROBERTS, W. M. (1994). Calcium-triggered exocytosis and endocytosis in an isolated presynaptic cell: capacitance measurements in saccular hair cells. *Neuron* **13**, 875–883.

PROKS, P. & ASHCROFT, F. M. (1995). Effects of divalent cations on exocytosis and endocytosis from single mouse pancreatic β-cells. *Journal of Physiology* **487**, 465–477.

PUSCH, M. & NEHER, E. (1988). Rates of diffusional exchange between small cells and a measuring patch pipette. *Pflügers Archiv* **411**, 204–211.

RAE, J., COOPER, K., GATES, P. & WATSKY, M. (1991). Low access resistance perforated patch recordings using amphotericin B. *Journal of Neuroscience Methods* **37**, 15–26.

REGAZZI, R., WOLLHEIM, C. B., LANG, J., THELER, J.-M., ROSSETTO, O., MONTECUCCO, C., SADOUL, K., WELLER, U., PALMER, M. & THORENS, B. (1995). VAMP-2 and cellubrevin are expressed in pancreatic β-cells and are essential for Ca^{2+}- but not for GTPγS-induced insulin secretion. *EMBO Journal* **14**, 2723–2730.

RORSMAN, P., BOKVIST, K., ÄMMÄLÄ, C., ELIASSON, L., RENSTRÖM, E. & GÄBEL, J. (1994). Ion channels, electrical activity and insulin secretion. *Diabete et Metabolisme* **20**, 138–145.

RORSMAN, P. & TRUBE, G. (1985). Glucose-dependent K^+-channels in pancreatic β-cells are regulated by intracellular ATP. *Pflügers Archiv* **405**, 305–309.

ROSENBOOM, H. & LINDAU, M. (1994). Exo-endocytosis and closing of the fission pore during endocytosis in single pituitary nerve terminals internally perfused with high calcium concentrations. *Proceedings of the National Academy of Sciences of the USA* **91**, 5267–5271.

THOMAS, P., LEE, A. K., WONG, J. G. & ALMERS, W. (1994). A triggered mechanism retrieves membrane in seconds after Ca^{2+}-stimulated exocytosis in single pituitary cells. *Journal of Cell Biology* **124**, 667–675.

THOMAS, P., WONG, J. G., LEE, A. K. & ALMERS, W. (1993). A low affinity Ca^{2+} receptor controls the final steps in peptide secretion from pituitary melanotrophs. *Neuron* **11**, 93–104.

VON GERSDORFF, H. & MATTHEWS, G. (1994). Inhibition of endocytosis by elevated internal calcium in synaptic terminal. *Nature* **370**, 652–655.

ZUCKER, R. (1994). Photorelease techniques for raising or lowering intracellular Ca^{2+}. *Methods in Cell Biology* **40**, 31–63.

Acknowledgements

Studies in the Oxford group were supported by grants from The Wellcome Trust, the British Medical Research Council and the British Diabetic Association. The studies in Göteborg were supported by the Juvenile Diabetes Foundation International, the Swedish Medical Research Council, the Swedish Diabetes Association, the Nordic Insulin Foundation Committee and the Magn. Bergvalls Stiftelse.

Author's permanent address

P. Proks: Institute of Molecular Physiology and Genetics, Vlarska 5, 833 34 Bratislava, Slovakia.

Received 19 December 1995; accepted 6 February 1996.